Composites: Part B xxx (2011) xxx–xxx

Contents lists available at SciVerse ScienceDirect

Composites: Part B

journal homepage: www.elsevier.com/locate/compositesb

Perforation of FRP laminates under impact by flat-nosed projectiles

Q.G. Wu, H.M. Wen *, Y. Qin, S.H. Xin

CAS Key Laboratory for Mechanical Behaviour and Design of Materials, University of Science and Technology of China, Hefei, Anhui Province 230027, China

ARTICLE INFO

Article history:
Received 21 March 2011
Received in revised form 9 May 2011
Accepted 22 August 2011
Available online xxxx

Keywords:
A. Laminates
B. Impact behaviour
C. Analytical modelling
Ballistic limit

ABSTRACT

A theoretical study is performed herein on the perforation of fibre-reinforced plastic laminates subjected to impact by flat-nosed projectiles in a wide range of velocities. Ballistic impact on FRP laminates is a very complex problem and it can be generally classified into two categories, i.e. global deformation with local rupture and wave-dominated local failure. Simple analytical models for both global deformation failure as well as wave-dominated local failure are first given, and a shear failure criterion is employed to predict the perforation of FRP laminates which fail in global deformation mode. By combining the wave-dominated local failure model and the concept of Von Karman's critical impact velocity, a condition for the transition of the above mentioned two failure modes is obtained. It is shown that the model predictions are in good agreement with available experimental observations in terms of ballistic limits and critical conditions for the transition of failure modes.

1. Introduction

Fibre-reinforced plastic (FRP) laminates have been extensively used in various industries such as aerospace, marine, transportation and defense because of their high specific strength and stiffness [1]. However, FRP laminates are vulnerable to localised transverse loads either static or impact due to their low fracture toughness of matrix materials [2]. Over the past several decades, a significant body of work has been focused on experimental and theoretical investigation on the transverse impact response of polymer matrix composite laminates in order to gain insight into their failure and energy absorption mechanisms.

Lee and Sun [3] and Sun and Potti [4] conducted a combined experimental and numerical study on the response and perforation of CFRP laminates under quasi-static and impact loading. Flat-nosed indenters/projectiles were employed in the tests with impact velocities ranging from 24 to 91 m/s. They considered that the process of penetration is composed of three stages: pre-delamination, post-delamination before plugging and post-plugging. On the basis of these three stages, a finite element model was formulated to simulate the static loading process and the load–displacement curve was adopted in the dynamic perforation analysis.

Greaves [5] investigated the failure mechanisms in ballistic perforation of thick S2-glass/phenolic laminated plates by cylindrical indenters and found that the failure was divided into two phases: phase I included compression, shear, indentation and expulsion of debris; phase II involved formation of a cone of delaminations, fibre stretching/fracture and the projectile exit from the distal side. It was noted that the phase I indentation mechanism, said to be dominated by the through-thickness compressive resistance of the material, absorbed most of the impact energy and was therefore worthy of more detailed study. To this end, an investigation into the impact force-indentation characteristics of laminates at velocities of up to 200 m/s has been carried out by Reid et al. [6].

Zhu et al. [7,8] conducted tests on the penetration of Kevlar-29/polyester laminates struck by conical-ended missiles and presented a series of models for various energy-absorbing mechanisms such as the indentation of projectile tip, the bulging of the back surface of the laminates, fibre failure, delamination and friction to estimate the target resistance to the projectile motion.

Xiao et al. [9] performed a comprehensive experimental and numerical research into the failure modes of GFRP laminates subjected to quasi-static punch shear. For thin FRP laminates, membrane stretching before local punch shear was observed and it was found that the dominant damage mechanisms were delamination and fibre breakage due to shear and tension. Gama and Gillespie [10] extended the work reported in [9] by conducting a full-fledged 3D FE simulations to investigate impact, damage evolution and penetration of thick-section composites under a wide range of impact velocities. Detailed damage and penetration mechanisms during two major phases of ballistic penetration (shock compression and penetration) were presented. Some other numerical simulations [11–13] were also carried out to study the damage and energy absorption of composite plates under impact by projectiles.

In a similar study, Jenq et al. [14] used the quasi-static punch curve to predict the ballistic limits of woven glass/epoxy laminates struck transversely by a hemispherical-tipped penetrator. Hoo Fatt

* Corresponding author. Tel.: +86 5513607740; fax: +86 5513606459.
E-mail address: hmwen@ustc.edu.cn (H.M. Wen).

1359-8368/$ - see front matter © 2011 Elsevier Ltd. All rights reserved.
doi:10.1016/j.compositesb.2011.08.045

Nomenclature

A_d (m^2) delamination area in the mid-plane
A_p (m^2) cross-sectional area of projectile
B empirical constant
C (m/s) sound speed in laminates along the fibre direction
C_{ij} (Pa) elastic constants
e_t (J/m^3) energy density for tensile tearing failure
E_1 (Pa) in-plane Young's moduli
$E3$ (Pa) through-thickness Young's moduli
E_{av} (Pa) average modulus $E_{av} = E_1$
E_{bm} (J) energy absorbed by the global deformation
E_{ct} (J) contact energy
E_{def} (J) total energy dissipation due to deformation
E_{del} (J) energy due to delamination
E_{frac} (J) energy dissipated by local failure
E_k (J) initial kinetic energy of projectile
E_p (J) impact perforation energy
E_T (J) quasi-static perforation energy
F (N) resistive force
G (kg) projectile mass
G_{13} (J) shear modulus
G_{IIc} (J/m^2) inter-laminar fracture toughness in Mode II
H_c (m) critical thickness of plate
H/D ratio of plate thickness to punch diameter
$(H/D)_c$ critical ratio of FRP laminate plate thickness to projectile diameter
K constraint factor
K_b (N/m) bending stiffness
K_{bs} (N/m) effective stiffness due to bending and shear
K_c (N/m) contact stiffness
K_m (N/m^3) membrane stiffness
K_s (N/m) shear stiffness
L (m) length of flat-faced projectile
P (N) quasi-static contact force
P_d (N) critical indenter load of delamination
r (m) radius of delamination area
R (m) radius of indenter/projectile
S (m) diameter or span of laminate plate
V_b (m/s) ballistic limit
V_c (m/s) Von Karman critical impact velocity
V_i (m/s) impact velocity of projectile
V_r (m/s) residual velocity of projectile
W_0 (m) transverse deflection of laminate plate
W_{0f} (m) critical transverse deflection of plate failure
W_t (m) total displacement of punch
α (m) local indentation
B empirical constant
ε_f static tensile failure strain
ν_{ij} Poisson's ratios
ρ_p (kg/m^3) density of flat-faced projectile
ρ_t (kg/m^3) density of laminate
σ_e (Pa) the linear elastic limit of FRP laminates in through-thickness compression
τ_{13} (Pa) transverse shear strength of plate
τ_{max} (Pa) maximum shear stress of mid-plane
τ_{IRSS} (Pa) inter-laminar shear stress
τ_0 (Pa) average shear stress
φ empirical constant
Φ dynamic enhancement factor

and Lin [2] proposed an analytical model based on classical membrane, bending and first order shear theories to analyse the deformation and damage of fully clamped panels.

Mines et al. [15] studied experimentally the high velocity perforation behaviours of fully clamped 200 mm × 200 mm polymeric composite laminates struck by flat, hemispherical and conical projectiles at impact velocities up to 571 m/s. Woven roving, z-stitched and through-thickness z-stitched glass polyester laminates for a number of laminate thickness (6, 12, 24 ply) were used in the tests. The results were presented in terms of static and impact perforation energies and energy absorption mechanisms during high velocity perforation were also discussed with a view to identifying improved combinations of materials.

Wen et al. [16–20] carried out an extensive investigation into the penetration and perforation of FRP laminates and sandwich panels with such laminates as skins and foam cores. It was observed experimentally that ballistic impact on FRP laminates can be classed into two categories: global response with local rupture and wave-dominated localised failure. Global response with local rupture is often associated with the behaviour of thin FRP laminates whilst wave-dominated localised failure with that of thick FRP laminates. Based on the assumption that the deformations are localised and the average resistance provided by target materials can be divided into two parts: quasi-static resistive pressure due to elastic–plastic deformations and dynamic resistive pressure arising from velocity effects. The dynamic resistive pressure is simply expressed as a velocity-dependent enhancement factor and related to the initial impact velocity. Subsequently, He et al. [21–23] modified the models proposed in [19,20] by assuming that the pressure provide by FRP laminates to resist the motion of a projectile is no longer a constant rather a function of penetration velocity. Various equations were obtained for the depth of penetration, residual velocity, and ballistic limit. Transient response was solved numerically in terms of time-histories of displacement/penetration, velocity and deceleration. It is found that the model predictions are in good agreement with available experimental data.

In this paper, a theoretical study is performed on the perforation of fibre-reinforced plastic laminates subjected to impact by flat-nosed projectiles in a wide range of velocities. Simple analytical equations for both global deformation failure as well as wave-dominated local failure are first given, and a shear failure criterion is used to predict the perforation of FRP laminates which fail in global deformation mode. By combining the wave-dominated local failure model and the concept of Von Karmen's critical impact velocity, a condition for the transition of the above mentioned two failure modes is obtained. The model predictions are compared with available experimental results and discussed.

2. Formulation of the problem

As noted previously, ballistic impact on FRP laminates can be divided into two categories, i.e. global deformation with local rupture and wave-dominated local failure. In the following sections, global deformation model is first presented, together with a shear failure criterion which can be used to predict the perforation of thin FRP laminates struck by a flat-nosed missile. By combining the wave-dominated local failure model suggested previously in [19,20] and the concept of Von Karman's critical impact velocity, a condition for the transition of the above mentioned two failure modes is then obtained.

2.1. Global deformation with local rupture

The perforation of thin FRP laminates stuck by a flat-ended projectile is a very complex problem which is impossible to be

Please cite this article in press as: Wu QG et al. Perforation of FRP laminates under impact by flat-nosed projectiles. Composites: Part B (2011), doi:10.1016/j.compositesb.2011.08.045

described theoretically by taking all the mechanisms into consideration. Therefore, the model described in the following is based on the assumption that local indentation, global bending and stretching, local shear/tensile tearing at the projectile–target interface, delaminations are the major energy absorbing mechanisms which are taken into account in the model development whilst other energy dissipating mechanisms such as friction are neglected.

2.1.1. Quasi-static load–displacement relationship

An FRP laminate plate loaded quasi-statically by a flat indenter at the centre (as shown schematically in Fig. 1) can be represented by the spring model shown in Fig. 2 [16,24]. As can be seen from Figs. 1 and 2 that the deformations of the laminate plate are assumed to consist of two parts: local indentation and global bending and stretching. K_c is a spring representing the contact stiffness and K_b, K_s and K_m are springs representing the bending, shear and membrane stiffness, respectively.

The quasi-static contact force, P, is related to the local indentation of the laminate plate, α, by an equation of the following form [16,25]

$$P = K_c\alpha \tag{1}$$

where $K_c = 2R/(\pi H_0)$ is the contact stiffness and R is the radius of the indenter. H_0 is defined by the following equations [16,25]:

$$H_0 = \frac{(\gamma_1+\gamma_2)C_{11}}{2\pi(C_{11}C_{33}-C_{13}^2)}, \quad \gamma_{1,2}^2 = Q \pm \sqrt{Q^2 - C_{33}/C_{11}}$$

$$Q = (C_{11}C_{33} - C_{13}^2 - 2C_{13}C_{44})/2C_{11}C_{44}$$

in which the coefficients C_{ij} are the elastic constants for a transversely isotropic elastic body. They are determined by elasticity theory and are given by

$$C_{11} = E_1/(1-\nu_{31}\nu_{12}), \quad C_{33} = E_3/(1-\nu_{31}\nu_{12}), \quad C_{44} = G_{13},$$
$$C_{13} = \nu_{12}E_1/(1-\nu_{31}\nu_{12})$$

where E_1 and E_3 are the in-plane and through-thickness Young's moduli, respectively; G_{13} is the shear modulus and ν_{12}, ν_{31} are the corresponding Poisson's ratios satisfying $\nu_{31} = \frac{E_3}{E_1}\nu_{12}$.

The load–deflection relation for the laminate plate ignoring the local indentation above may be written as [16,24]

$$P = K_{bs}W_0 + K_mW_0^3 \tag{2}$$

where W_0 is the transverse deflection of the mid-plane of the plate, K_{bs} and K_m are the effective stiffness due to bending and shear and the membrane stiffness, respectively. The expressions for bending stiffness K_b and membrane stiffness K_m were derived using the Babunov-Galerkin methodology. For the fully clamped plate K_b and K_m are given by the following equations [24,26]:

$$K_b = \frac{86.2E_1H^3}{12(1-\upsilon_{12}^2)S^2} \quad \text{for a square laminate plate} \tag{3}$$

$$K_b = \frac{16\pi E_1H^3}{3(1-\upsilon_{12}^2)S^2} \quad \text{for a circular laminate plate} \tag{4}$$

$$K_m = \frac{191\pi E_1H}{162S^2} \tag{5}$$

K_{bs} is given by

$$K_{bs} = \frac{K_bK_s}{K_b+K_s} \tag{6}$$

The effective shear stiffness is given by [24]

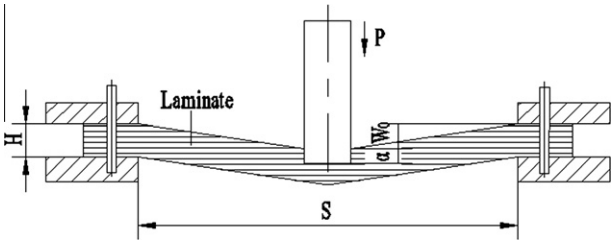

Fig. 1. Schematic diagram of an FRP laminate plate loaded by a flat punch.

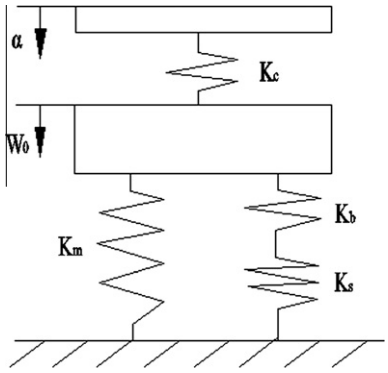

Fig. 2. The spring model.

$$K_s = \frac{4\pi}{3}G_{13}H\left(\frac{E_1}{E_1-4\nu_{12}G_{13}}\right)\left(\frac{4}{3}+Log\frac{S}{2R}\right)^{-1} \tag{7}$$

where S is the diameter or span of the laminate plate. The total displacement of the punch is $W_t = W_0 + \alpha$. Hence, combining Eqs. (1) and (2) with $W_t = W_0 + \alpha$ gives the quasi-static load–displacement relationship, viz.

$$P = f(W_t) \tag{8}$$

2.1.2. Energy absorption

It is constructive to calculate and compare the energies dissipated by each mechanism during laminate plate perforation. Mines et al. [15] also carried out energy calculations of the clamped GRP laminates, three modes of energy absorption were identified, namely, local perforation, delamination and friction between the projectile and the laminates. In their energy calculation, however, global deformation was ignored, which was observed experimentally for relatively thin GRP laminates. In the following, various energy terms are derived which are dissipated by local indentation, global deformation, shearing plugging or localised tensile fracture and delaminations.The contact energy (E_{ct}) is given by the following equation, viz.

$$E_{ct} = \int_0^{\alpha} Pd\alpha = \frac{1}{2}K_c\alpha^2 = \frac{P^2}{2K_c} = \frac{\left(K_{bs}W_0 + K_mW_0^3\right)^2}{2K_c} \tag{9}$$

The energy absorbed by the global deformation is

$$E_{bm} = \int_0^{W_0} PdW_0 = \frac{1}{2}K_{bs}W_0^2 + \frac{1}{4}K_mW_0^4 \tag{10}$$

The total energy dissipation due to deformations can therefore be written as

$$E_{def} = \frac{\left(K_{bs}W_0 + K_mW_0^3\right)^2}{2K_c} + \frac{1}{2}K_{bs}W_0^2 + \frac{1}{4}K_mW_0^4 \tag{11a}$$

Please cite this article in press as: Wu QG et al. Perforation of FRP laminates under impact by flat-nosed projectiles. Composites: Part B (2011), doi:10.1016/j.compositesb.2011.08.045

or

$$E_{def} = \frac{\left(K_{bs}W_{0f} + K_m W_{0f}^3\right)^2}{2K_c} + \frac{1}{2}K_{bs}W_{0f}^2 + \frac{1}{4}K_m W_{0f}^4 \quad (11b)$$

where W_{0f} is the critical transverse deflection at which plate failure occurs and, to a first approximation, it can be determined by the following equation [16]:

$$P = K_{bs}W_{of} + K_m W_{of}^3 = 2\pi RHK\tau_{13} \quad (12)$$

where τ_{13} is the transverse shear strength of the laminate plate and K is a constraint factor. During indentation, the deformation of the material in the neighbourhood will lead to the average transverse shear strength greater than the real material property. For simplicity K is taken as 2 in this paper [16].

It has been observed experimentally that an FRP laminate plate loaded by a flat-faced punch will fail either by local shear plugging or by mixed mode of local shear and tensile tearing (upper part of the laminate plate fails by shear and its lower part by tensile tearing) depending on the ratio of plate thickness to punch diameter (H/D). When H/D is greater than a critical value (φ) the plate will fail by mixed mode, otherwise it will fail by local shear plugging. Hence, the energy dissipated by local failure can be written as

$$E_{frac} = \pi R^2(H - \varphi D)e_t + \pi R(\varphi D)^2 K\tau_{13} \quad (\text{for } H/D > \varphi) \quad (13a)$$

or

$$E_{frac} = \pi RH^2 K\tau_{13} \quad (\text{for} H/D \le \varphi) \quad (13b)$$

where e_t is the energy density for tensile tearing failure and φ is an empirical constant which can be taken to be 0.21 approximately [27].

Delamination initiates below the contact loading area by coalescence of matrix cracks at interfaces with high inter-laminar shear stresses. It can propagate under Mode I (tensile) and Mode II (shear) loading and the relative importance of each mode is dependent on the structural configuration as well as the material properties. Frost [28] and Zee and Hsieh [29] suggested that, for projectile impact on FRP laminates, propagation is dominated by G_{IIC}. The energy due to delamination can be expressed as

$$E_{del} = A_d \times G_{IIC} \quad (14)$$

where A_d is the delamination area in the mid-plane and G_{IIC} is the inter-laminar fracture toughness in Mode II. Davies and Zhang [30] proposed that a single central delamination in the plate's mid-plane will propagate in Mode II at a critical force given by

$$P_d^2 = \frac{8\pi^2 E_{ev} H^3 G_{IIC}}{9(1 - v_{12}^2)} \quad (15)$$

where E_{av} is the average modulus. For transversely isotropic FRP laminates, E_{av} can be taken as E_1.

When the indenter load reaches the critical load of the delamination, the critical inter-laminar shear stress can be estimated. The through-thickness shear stress varies from zero at the surfaces to a maximum at the mid-plane parabolically, as shown schematically in Fig. 3, so the actual shear stress through the thickness can be related to the maximum shear stress τ_{max} as $\tau_{rz} = \tau_{max}\left[1 - \left(\frac{2z}{H}\right)^2\right]$. Equilibrium of the applied load with the resultant force from uniformly distributed or average shear stress τ_0 yields $\tau_0 = \frac{P}{2\pi rH}$ with r beings the radius of the delamination area. We can easily get the average shear stress, i.e. $\tau_0 = \frac{2}{3}\tau_{max}$ and the maximum shear stress of the mid-plane is $\tau_{max} = \frac{3P}{4\pi rH}$.

When the inter-laminar shear stress is greater than the critical value of τ_{IRSS}, the delamination radius is determined by the following equation:

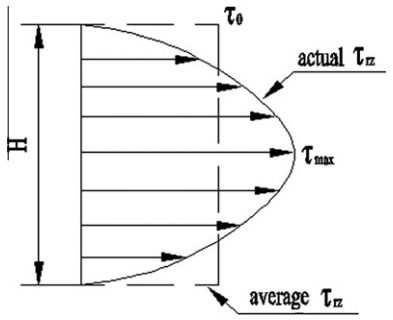

Fig. 3. Schematic diagram of inter-laminar shear stress distribution.

$$r = \frac{3P_d}{4\pi H\tau_{IRSS}} \quad (16)$$

Thus, the total delamination area is calculated by

$$A_d = \pi r^2 = \frac{9}{16\pi H^2}\left(\frac{P_d}{\tau_{IRSS}}\right)^2 \quad (17)$$

Hence, the energy due to delamination is given by

$$E_{del} = \frac{9}{16\pi H^2}\left(\frac{P_d}{\tau_{IRSS}}\right)^2 G_{IIC} \quad (18)$$

The total energy dissipated in the perforation of an FRP laminate plate loaded quasi-statically by a flat indenter at the centre can therefore be written as

$$E_T = E_{def} + E_{frac} + E_{del} \quad (19)$$

2.1.3. Dynamic enhancement factor and ballistic limit

It is assumed that the energy absorbing mechanisms in an impact problem are the same as those in corresponding quasi-static one. Hence, the impact perforation energy (E_P) may be written as [16]

$$E_P = \Phi E_T \quad (20a)$$

in which E_T is the quasi-static perforation energy estimated by Eq. (19) and Φ is the dynamic enhancement factor which may be expressed as [16]

$$\Phi = \begin{cases} 1 + B\left(\frac{V_i}{V_c}\right) & (V_i < V_c) \\ 1 + B & (V_i > V_c) \end{cases} \quad (20b)$$

where B is an empirical constant and V_c is the Von Karman critical impact velocity which is given by [16]

$$V_c = C\varepsilon_f = \sqrt{\frac{E_1}{\rho_t}}\varepsilon_f \quad (21)$$

in which C is the sound speed in the laminates along the fibre direction, ρ_t and E_1 are the density and the in-plane Young's modulus of the laminates, respectively. From Eqs. (20a) and (19) one obtains an approximate value for the ballistic limit (V_b), viz.

$$V_b = \sqrt{\frac{2\Phi(E_{def} + E_{frac} + E_{del})}{G}} \quad (22)$$

after using $E_P = \frac{1}{2}GV_b^2$ where G is the projectile mass. E_{def}, E_{frac} and E_{del} are evaluated by Eqs. (11b), (13) and (18), respectively. To a first approximation, the residual velocity of the projectile (V_r) can be estimated by

$$V_r = \sqrt{V_i^2 - V_b^2} \quad (23)$$

where V_i is the impact velocity of the projectile.

Please cite this article in press as: Wu QG et al. Perforation of FRP laminates under impact by flat-nosed projectiles. Composites: Part B (2011), doi:10.1016/j.compositesb.2011.08.045

2.2. Wave-dominated local response

Wave-dominated local response of FRP laminates subjected to impact by projectiles with different nose shapes has been examined by Wen et al. [19–23]. For the sake of completeness some of the main results are quoted as follows.

The pressure offered by an FRP laminate plate to resist the motion of a projectile can be expressed as [19,20]

$$\sigma = \sigma_e + \beta\sqrt{\rho_t \cdot \sigma_e} \cdot V_i \tag{24}$$

where σ_e is the linear elastic limit of the FRP laminates in through-thickness compression and V_i is the initial impact velocity of the projectile. β is an empirical constant (for flat-nosed missiles $\beta = 2$).

The resistive force of a flat-ended projectile exerted by an FRP laminate target can be written as

$$F = \sigma A_p = \frac{1}{4}\pi D^2 \sigma \tag{25}$$

where F is the resistive force and A_p is the cross-sectional area of the projectile. Substituting Eq. (24) into Eq. (25) gives

$$F = \frac{\pi D^2}{4}\left(\sigma_e + \beta\sqrt{\rho_t \sigma_e} V_i\right) \tag{26}$$

From energy balance, one obtains

$$E_k = F \cdot H = \frac{\pi D^2 H}{4}\left(\sigma_e + \beta\sqrt{\rho_t \sigma_e} V_i\right) \tag{27}$$

Substituting $E_k = \frac{1}{2}GV_b^2$ and $V_i = V_b$ into the above equation and rearranging yields an approximate value for the ballistic limit, i.e.

$$V_b = \frac{\pi\sqrt{\rho_t \sigma_e} D^2 H}{2G}\left[1 + \sqrt{1 + \frac{2G}{\pi \rho_t D^2 H}}\right] \tag{28}$$

2.3. Critical condition for the transition from global deformation to local response

As noted previously, the perforation of FRP laminates subjected to impact by flat-nosed missiles can be divided into two categories, i.e. global deformation with local rupture and wave-dominated local failure. It has to be mentioned here that ballistic impact on FRP laminates is a very complex problem and the failure mode in which the laminates fail can be affected by many factors such as projectile diameter, projectile mass, target thickness, target span and the projectile's impact velocity. In the following a critical condition for the transition of the above mentioned two failure modes is derived in a pragmatic way by combining the wave-dominated local response model given in Section 2.2 and the concept of Von Karman's critical impact velocity.

It is assumed here that if an FRP laminate plate under impact by a flat-nosed projectile fails in wave-dominated local response mode then its ballistic limit should not be less than Von Karman's critical impact velocity, namely, $V_b \geqslant V_c$. Substituting $V_b = V_c = \sqrt{E_1/\rho_t}\varepsilon_f$ into Eq. (28) and rearranging gives the critical ratio of FRP laminate plate thickness to projectile diameter $(H/D)_c$, viz.

$$\left(\frac{H}{D}\right)_c = \frac{\varepsilon_f^2}{2\left[1 + 2\sqrt{E_1/\sigma_e}\varepsilon_f\right]}\left(\frac{E_1}{\sigma_e}\right)\left(\frac{\rho_p}{\rho_t}\right)\left(\frac{L}{D}\right) \tag{29}$$

after using $G = \frac{1}{4}\pi D^2 L\rho_p$ with ρ_p and L being the density and the length of the flat-faced projectile, respectively. The physical meaning of Eq. (29) is this: if $H/D \geqslant (H/D)_c$ then the FRP laminate plate will fail in wave-dominated local response mode, otherwise it will fail in a mode characterised by global deformation with local rupture.

3. Comparisons with available test results and discussion

In this section, the model predictions are compared with the test data reported in Refs. [3,5,31,33]. In the theoretical calculations the values of various parameters for the FRP laminate plates examined are listed in Table 1. The values of the majority of parameters are obtained from the literatures [2,3,15,16,31–33] and the value of a parameter unavailable in the literature is obtained by the rule of mixture.

Fig. 4 shows comparisons of the model predictions with the experimental data obtained by Mines et al. [15]. The critical ratio $(H/D)_c$ is calculated using Eq. (29) to be 0.168 for GFRP laminates struck by a 6 g, 7.6 mm diameter flat-nosed projectile.

It is clear from Fig. 4 that the global deformation failure model underpredicts the ballistic limits and that the discrepancy between the predicted results (Eq. (22)) and the experimental data increases with increasing ratio (H/D) of plate thickness to projectile diameter. It is also clear from Fig. 4 that the wave-dominated local failure model (Eq. (28)) agrees reasonably well with the experimental data. This is not surprising since the thicknesses of the GFRP laminates tested are greater than the critical thickness (H_c) predicted by the present model (Eq. (29)). In other words, wave-dominated local response plays a dominant role in the failure of all the GFRP laminates examined in [15]. It should be mentioned here that the average fibre volume fraction of the GRP laminates examined in [15] is slightly higher than that of the GRP laminates investigated in [16]. If the real value of σ_e for the laminates is used better agreement should be obtained between the model predictions and the experimental data.

Fig. 5 shows comparisons of the model predictions with the experimental data reported in Ref. [31]. The critical ratio $(H/D)_c$ is calculated using Eq. (29) to be 0.160 for GFRP laminates struck by a 3.84 g, 6.35 mm diameter flat-ended projectile.

It is evident from Fig. 5 that the predictions from the wave-dominated local failure model are in good agreement with the experimental results whilst the global deformation failure model underpredicts the ballistic limits. It is also evident from Fig. 5 that the differences between the test data and the predicted values by the global deformation failure model increases with increasing plate thickness. This trend observed in Fig. 5 for the GFRP laminates investigated in [31] is similar to that in Fig. 4 for the GFRP laminates studied in [15].

Fig. 6 shows comparisons of the model predictions with the experimental data obtained by Lee and Sun [3]. The critical ratio $(H/D)_c$ is calculated using Eq. (29) to be 0.287 for CFRP laminates struck by 30 g, 14.5 mm diameter flat-ended projectiles. This implies that all the CFRP laminates with thicknesses less than the critical thickness ($H_c = 4.16$ mm) should fail by global deformation

Table 1
Properties of FRP laminate plates.

	E-glass/epoxy [15]	E-glass/vinylester [31]	Graphite/epoxy [3]	Carbon/epoxy [33]
S	200 mm	100 mm	43.5 mm	101.6 mm
ρ_t	1650 kg/m^3	1850 kg/m^3	1550 kg/m^3	1550 kg/m^3
E_1	23.1 GPa	24.9 GPa	53.7 GPa	53.7 GPa
E_3	6.87 GPa	7.4 GPa	11.7 GPa	11.7 GPa
G_{13}	1.8 GPa	1.9 GPa	4 GPa	4 GPa
υ_{12}	0.15	0.15	0.31	0.31
τ_{13}	45 MPa	49 MPa	79 MPa	79 MPa
ε_f	0.021	0.021	0.0138	0.0138
τ_{IRSS}	13 MPa	13 MPa	50 MPa	50 MPa
e_t	4.23 MJ/m^3	4.98 MJ/m^3	5.1 MJ/m^3	5.1 MJ/m^3
G_{IIC}	2.8 kJ/m^2	2.8 kJ/m^2	0.8 kJ/m^2	0.8 kJ/m^2
B	1.64	1.64	0	0
φ	0.21	0.21	0.21	0.21
σ_e	225 MPa	250 MPa	85 MPa	85 MPa

Please cite this article in press as: Wu QG et al. Perforation of FRP laminates under impact by flat-nosed projectiles. Composites: Part B (2011), doi:10.1016/j.compositesb.2011.08.045

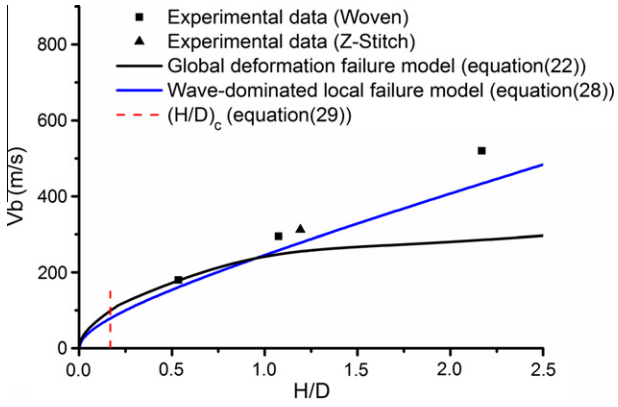

Fig. 4. Comparison between the model predictions and the experimental results for the ballistic limits of GFRP laminates struck transversely by a 6 g, 7.6 mm diameter flat-nosed projectile [15].

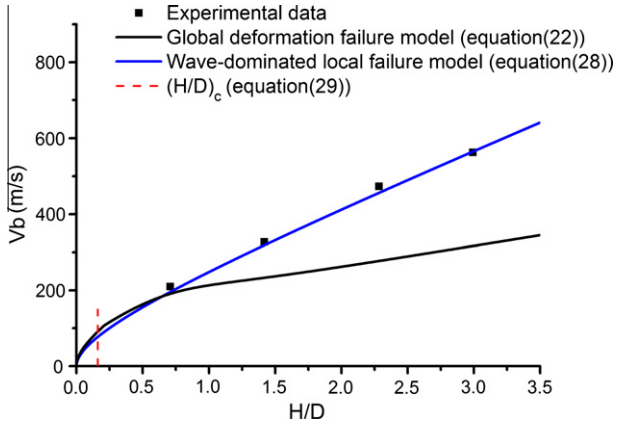

Fig. 5. Comparison between the model predictions and the experimental results for the ballistic limits of GFRP laminates struck transversely by a 3.84 g, 6.35 mm diameter flat-nosed projectile [31].

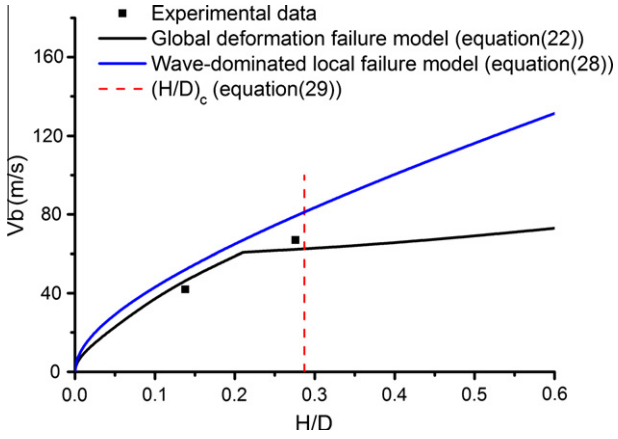

Fig. 6. Comparison between the model predictions and the experimental results for the ballistic limits of CFRP laminates struck normally by a 30 g, 14.5 mm diameter flat-nosed projectile [3].

failure mode. Indeed, as can be seen from Fig. 6 that the global deformation failure model (Eq. (22)) is in good agreement with the test data whilst the wave-dominated local failure model (Eq. (28)) overpredicts the ballistic limits.

Fig. 7 shows comparisons of the model predictions with the experimental data obtained by Ulven et al. [33]. The critical ratio

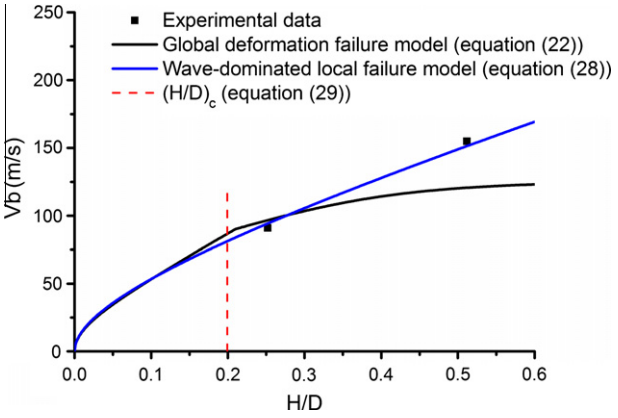

Fig. 7. Comparison between the model predictions and the experimental results for the ballistic limits of CFRP laminates struck normally by a 14 g, 12.7 mm diameter flat-ended projectile [33].

$(H/D)_c$ is calculated using Eq. (29) to be 0.199 for CFRP laminates struck by 14 g, 12.7 mm diameter flat-ended projectiles.

The CFRP laminates tested with the flat-nosed projectile have thicknesses of 3.2 mm and 6.5 mm which are greater than the critical thickness (H_c = 2.53 mm) predicted by Eq. (29). In other words, these two laminates should fail by wave-dominated local failure mode according to the present model suggested in the previous section. Indeed, as can be seen from Fig. 7 that the wave-dominated local failure model (Eq. (28)) is in good agreement with the experimental results. It should be mentioned here that in Ref. [33] Ulven et al. used the compressive strength of the CFRP laminates in through-thickness direction rather than the linear elastic limit as defined by Wen in his original work [19,20] to calculate the ballistic limits. That is why in their paper Wen's model using σ_e = 211 MPa overpredicts the ballistic limits by a large margin compared to the test results. In the present theoretical calculations the linear elastic limit of the CFRP laminates in the through-thickness compression, i.e. σ_e = 85 MPa is employed instead. This value is obtained from the stress–strain curve in through-thickness compression of a similar CFRP laminates reported in Ref. [32].

Generally speaking, there are two failure modes, i.e. the global deformation failure mode and the wave-dominated local failure mode compete each other in the perforation of an FRP laminate plate struck normally by a flat-ended projectile and which mode predominates depending upon the combinations of various parameters as dictated by Eq. (29). For the combination of a given flat-faced missile and an FRP laminate plate Eq. (29) can tell us in what mode the FRP laminate plate will fail, namely, if $H/D \geqslant (H/D)_c$ then the FRP laminate plate will fail in wave-dominated local response mode, otherwise it will fail in a mode characterised by global deformation with local rupture. Furthermore, the ballistic limit can be computed from the corresponding equation (i.e. Eq. (28) if it fails in wave-dominated local failure mode or Eq. (22) if it fails in global deformation mode).

As for non-flat-nosed projectiles the methodology described above should also apply and the results will be published in a subsequent paper.

4. Conclusions

A theoretical study has been conducted on the perforation of fibre-reinforced plastic laminates subjected to impact by flat-nosed projectiles in a wide range of velocities. Ballistic impact on FRP laminates can be categorised into either the global deformation with local rupture or wave-dominated local failure. In the global deformation model, a quasi-static approach was used to predict

Please cite this article in press as: Wu QG et al. Perforation of FRP laminates under impact by flat-nosed projectiles. Composites: Part B (2011), doi:10.1016/j.compositesb.2011.08.045

the energy absorption, which includes global deformation energy, local fracture energy and delamination energy. Furthermore, it is assumed that the energy absorbing mechanisms in an impact problem are similar to those in a corresponding quasi-static one, hence, the impact perforation energy can be predicted by the quasi-static energy multiplied by a dynamic enhancement factor. By combining the wave-dominated local failure model suggested previously and the concept of Von Karman's critical impact velocity, a condition for the transition of the above mentioned two failure modes is obtained.

It is shown that the model predictions are in good agreement with available experimental observations in terms of ballistic limits and critical conditions for the transition of failure modes.

References

[1] Abrate S. Impact on composite structures. Cambridge, UK: Cambridge University Press; 1998.
[2] Hoo Fatt MS, Lin CF. Perforation of clamped, woven E-glass/polyester panels. Composites Part B 2004;35(5):359–78.
[3] Lee SWR, Sun CT. Dynamic penetration of graphite/epoxy laminates impacted by a blunt ended projectile. Compos Sci Technol 1993;49(4):369–80.
[4] Sun CT, Potti SV. A simple model to predict residual velocities of thick composite laminates subjected to high velocity impact. Int J Impact Eng 1996;18(3):339–53.
[5] Greaves LJ. Progress in modeling the perforation of GFRP by ballistic projectiles. Unpublished UK DRA report; 1994.
[6] Reid SR, Reddy TY, Ho HM, et al. Dynamic indentation of thick fibre-reinforced composites. In: Rajapakse YDS, Vinson JR, editors. High strain rate effects on polymer, metal and ceramic matrix composites and other advanced materials, vol. 48. ASME AD; 1995. p. 71–9.
[7] Zhu G, Goldsmith W, Dharan CKH. Penetration of laminated Kevlar by projectiles – I. Experimental investigation. Int J Solids Struct 1992;29(4):399–420.
[8] Zhu G, Goldsmith W, Dharan CKH. Penetration of laminated Kevlar by projectiles – II. Analytical model. Int J Solids Struct 1992;29(4):421–36.
[9] Xiao JR, Gama BA, Gillespie JW. Progressive damage and delamination in plain weave S-2 glass/SC-15 composites under quasi-static punch–shear loading. Compos Struct 2007;78(2):182–96.
[10] Gama BA, Gillespie Jr JW. Finite element modeling of impact, damage evolution and penetration of thick-section composites. Int J Impact Eng 2011;38(4):181–97.
[11] Bouvet C, Castanié B, Bizeul M, Barrau J. Low velocity impact modelling in laminate composite panels with discrete interface elements. Int J Solids Struct 2009;46(14–15):2809–21.
[12] Sheikh AH, Bull PH, Kepler JA. Behavior of multiple composite plates subjected to ballistic impact. Compos Sci Technol 2009;69(6):704–10.
[13] Gower HL, Cronin DS, Plumtree A. Ballistic impact response of laminated composite panels. Int J Impact Eng 2008;35(9):1000–8.
[14] Jenq ST, Jing HS, Chung C. Predicting the ballistic limit for plain woven glass/epoxy composite laminate. Int J Impact Eng 1994;15(4):451–64.
[15] Mines RAW, Roach AM, Jones N. High velocity perforation behavior of polymer composite laminates. Int J Impact Eng 1999;22(6):561–88.
[16] Wen HM, Reddy TY, Reid SR, Soden PD. Indentation, penetration and perforation of composite laminates and sandwich panels under quasi-static and projectile loading. Key Eng Mater 1998;141–143:501–52.
[17] Reddy TY, Wen HM, Reid SR, Soden PD. Penetration and perforation of composite sandwich panels by hemispherical and conical projectiles. Trans ASME J Pres Ves Technol 1998;120(2):186–94.
[18] Reid SR, Wen HM, Soden PD, Retty TY. Response of single skin laminates and sandwich panels to projectile impact. In: Wang SS, Williams JJ, Lo KH, editors. Composite materials for offshore operation-2. Amer. Bur. Shipp.; 1999. p. 593–617.
[19] Wen HM. Predicting the penetration and perforation of FRP laminates struck normally by projectiles with different nose shapes. Compos Struct 2000;49(3):321–9.
[20] Wen HM. Penetration and perforation of thick FRP laminates. Compos Sci Technol 2001;61(8):1163–72.
[21] He T, Wen HM, Qin Y. Penetration and perforation of FRP laminates struck transversely by conical-nosed projectiles. Compos struct 2007;81(2):243–52.
[22] He T, Wen HM, Qin Y. Ballistic penetration and perforation of thick FRP laminates by ogival-nosed projectiles. J Compos Mater 2007;41(23):2829–42.
[23] He T, Wen HM, Qin Y. Finite element analysis to predict penetration and perforation of thick FRP laminates struck by projectiles. Int J Impact Eng 2008;35(1):27–36.
[24] Shivakumar KN, Elber W, Illg W. Prediction of impact force and duration due to low velocity impact on circular composite laminates. J Appl Mech 1985;52(3):674–80.
[25] Fabrikant VI, Selvadurai APS, Xistris GD. Asymmetric problem of loading under a smooth punch. J Appl Mech 1985;52(3):681–5.
[26] Timonshenko SP, Woinowsky-Krieger S. Theory of plates and shells. 2nd ed. New York: Mcgraw Hill; 1961.
[27] Qin Y. Theoretical and numerical study on failure modes of FRP laminates struck normally by projectiles. MSC Dissertation, University of Science and Technology of China; 2009.
[28] Frost SR. The impact behavior and damage tolerance of filament wound glass fiber/epoxy matrix pipes. In: 6th International conference on Fibre Reinforced Composites (FRC 94). Newcastle-upon-Tyne, United Kingdom; March 29–31, 1994. p. 3.1–3.10.
[29] Zee RH, Hsieh CY. Energy loss partitioning during ballistic impact of polymer composites. Polym Compos 1993;14(3):265–71.
[30] Davies GAO, Zhang X. Impact damage prediction in carbon composite structures. Int J Impact Eng 1995;16(1):149–70.
[31] Gellert EP, Cimpoeru SJ, Woodward RL. A study of the effect of target thickness on the ballistic perforation of glass–fibre-reinforced plastic composites. Int J Impact Eng 2000;24(5):445–56.
[32] Soden PD, Hinton MJ, Kaddour AS. Lamina properties, lay-up configurations and loading conditions for a range of fiber-reinforced composite laminate. Compos Sci Technol 1998;58(7):1011–22.
[33] Ulven C, Vaidya UK, Hosur MV. Effect of projectile shape during ballistic perforation of VARTM carbon/epoxy composite panels. Compos Struct 2003;61(1–2):143–50.

Please cite this article in press as: Wu QG et al. Perforation of FRP laminates under impact by flat-nosed projectiles. Composites: Part B (2011), doi:10.1016/j.compositesb.2011.08.045